



Microwave-assisted preparation and characterization of organo-attapulgites and comparison for 1-naphthol removal: equilibrium, kinetic, and thermodynamic studies

Yanfang Tai^{a,b,*}, Chunjie Shi^{a,b}, Guanghui Li^a, Jingmei Wu^a

^aSchool of Applied Chemistry and Environmental Engineering, Bengbu College, Bengbu 233030, Anhui, P.R. China, Tel. +86 552 3171286; emails: 88158197@qq.com (Y. Tai), 445679134@qq.com (C. Shi), 635294295@qq.com (G. Li), 951170372@qq.com, bbxywjim@126.com (J. Wu)

^bSchool of Chemical Engineering, Hefei University of Technology, Hefei 230009, Anhui, P.R. China

Received 26 July 2013; Accepted 23 April 2015

ABSTRACT

In this study, Na-attapulgite (Na-APT) was modified with octadecyl trimethyl ammonium chloride (OTMAC), sodium dodecyl sulfate (SDS), and the mixture of OTMAC and SDS using microwave-assisted technique. The prepared organo-attapulgites were characterized in detail. The combined analysis of characterizations indicated that surfactants were successfully introduced on the surfaces of attapulgite. A batch technique was adopted to investigate the removal efficiency of organo-attapulgites toward 1-naphthol under environmental conditions. The results showed that pseudo-second-order model and intraparticle diffusion model simulated the adsorption kinetic data better than that of pseudo-first-order model. The adsorption of 1-naphthol by organo-attapulgites fit reasonably well to Langmuir, Freundlich, and linear isothermal models. The negative values of ΔG° and ΔH° obtained from thermodynamic study indicated the spontaneous and exothermic nature of 1-naphthol adsorption on Na-APT and organo-attapulgites. Based on the experimental results, it could be deduced that the mechanism of 1-naphthol removal was a combination of surface adsorption and partitioning mechanism. The maximum adsorption capacity of organo-attapulgites for 1-naphthol was in the sequence of OTMAC/SDS-APT > OTMAC-APT > SDS-APT, which suggested that OTMAC/SDS-APT could be potentially used as a cost-effective material for the purification of actual organic contaminants-bearing effluents.

Keywords: Organo-attapulgite; 1-naphthol; Adsorption; Microwave-assisted technique; Removal mechanism

1. Introduction

Widespread contamination of surface water and groundwater with synthetic aromatic compounds is one of the most serious environmental problems that

we encountered recently [1]. 1-naphthol, often discharged from industries related with medicine, dye-stuff, photograph, and agrochemical industries [2,3], is of particular concern due to its acute toxicity, low biodegradation, and negative environmental impacts. Various technologies have been used for the removal of organic pollutants from aqueous solutions,

*Corresponding author.

including adsorption [4–6], oxidative degradation [7,8], photolysis [9], and biodegradation [10]. Among those technologies, adsorption is the most eco-friendly and economical method, which has been widely employed for the removal of organic pollutants from aqueous solutions [11]. Carbonaceous adsorbents, such as activated carbon [12], multiwalled carbon nanotubes (MWCNTs) [13], and graphene [14] have been investigated to decontaminate organic pollutants from aqueous solutions, and the experimental results demonstrate that carbonaceous adsorbents possess high adsorption capacities. However, carbonaceous adsorbents suffer from high cost, which restricts their applications in wastewater treatment.

Attapulgite is a hydrated magnesium silicate, which exists in nature as a fibrous clay mineral with a structure consisting of parallel ribbons of 2:1 layers. It has a rough surface, resulting in a relatively high surface area and moderate cation exchange capacity (CEC) [15]. The isomorphous substitutions of Al^{3+} for Si^{4+} in the tetrahedral layer result in a net negative surface charge on the clay. It is shown that attapulgite is applicable for the removal of a number of inorganic and organic pollutants from wastewater, including heavy metals [16], radionuclides [17], and dyestuffs [18]. Because the surface of attapulgite is hydrophilic in nature, thus, the surface of attapulgite is expected to have little affinity toward other hydrophobic organic pollutants such as ionizable and non-ionizable organic pollutants. However, the surface properties of attapulgite can be greatly modified with surfactants, so that the attapulgite can be hydrophobic and better retain organic pollutants [19–21]. Surfactants have complex effects on the behavior of other contaminants by solubilization, catalysis, and interfere in the removal processes of insoluble/soluble substances [22]. Tan et al. have studied counterion effects of nickel and sodium dodecylbenzene sulfonate adsorption to MWCNTs in aqueous solution and revealed that the adsorbed SDBS on MWCNTs could lead to the modification of the MWCNT surfaces and partial complexation of nickel with SDBS adsorbed on MWCNTs [23]. Similar observation could be also found on the effect of surfactants on Pb(II) adsorption from aqueous solutions using MWCNTs [24].

Up to now, researches on the organic modification of attapulgite mainly focus on attapulgite modified by the alkyl quaternary ammonium cationic surfactant such as dodecyltrimethylammonium and cetyltrimethylammonium, since cationic surfactant is easy to be adsorbed on the surfaces of clay, thus the surface properties of attapulgite can be changed obviously [25]. However, anionic surfactant is difficult to be adsorbed on the clay surfaces which due to its

negative charge. Interestingly, Zhu and Chen [26] have adopted the mixture of cationic surfactant and anionic surfactant to modify the surface properties of bentonite, another common clay mineral, and they found that the mixture of anionic and cationic surfactants could form mixed micelles, which could produce synergies solubilization to organic compounds. According to our literature survey, few researches focus on the modification of attapulgite using anionic and cationic surfactants simultaneously [27], and there is little information available in the literature about the comparison of 1-naphthol adsorption on organo-attapulgites modified with different surfactants, such as octadecyl trimethyl ammonium chloride (OTMAC), sodium dodecyl sulfate (SDS), and the mixture of OTMAC and SDS.

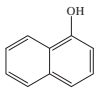
In our present work, Na-attapulgite (Na-APT) was modified with OTMAC, SDS, and the mixture of OTMAC and SDS, respectively. Microwave-assisted technique was used to prepare the organo-attapulgites. Compared with the conventional methods, such as conventional stirring treatment [28], the microwave-assisted technique is a more environmentally friendly and highly efficient method with the advantages of rapid volumetric heating, high reaction rate, short reaction time, enhanced reaction selectivity, and energy saving [29]. The prepared organo-attapulgites were characterized by a combined analysis of elemental analysis, X-ray powder diffraction (XRD), Fourier transform infrared spectroscopy (FT-IR), scanning electron microscopy (SEM), N_2 adsorption-desorption, and zeta potential measurement. Then the organo-attapulgites were employed for the removal of 1-naphthol from aqueous solutions. The adsorption equilibrium, kinetics, and thermodynamics were investigated in detail. This work aimed at adsorption comparison for 1-naphthol among Na-APT and three different organo-attapulgites, and further discussions about the corresponding mechanisms of 1-naphthol removal from aqueous solutions were involved in the process.

2. Materials and methods

2.1. Materials

SDS, OTMAC, 1-naphthol, and other chemical reagents were purchased from Sinopharm Chemical Reagent Co., Ltd., (Shanghai, China) in analytical purity and used directly without any further purification. SDS and OTMAC were used as the anionic and cationic surfactants to modify the attapulgite surface. All the reagents were prepared with deionized water. 1-naphthol was used as an adsorbate and its selected properties were listed in Table 1. The sample of

Table 1
Chemical structure and selected properties of 1-naphthol applied in this study^a

Chemical structure	M	S	K _{ow}	BP	MP	pK _a
1-naphthol 	144.17	866	501	555	328	9.34

Notes: M: molecular weight, g mol⁻¹; S: aqueous solubility, mg L⁻¹; K_{ow}: octanol–water partition coefficient; BP and MP are boiling and melting point temperature (unit is K), respectively; pK_a: acid dissociation constant.

^aRef. [13].

natural attapulgite was obtained from Xuyi county (Jiangsu, China). The natural attapulgite is not pure and contains some components as non-attapulgite fractions, which involves quartz and montmorillonite, as well as other metal oxides (Table 2). It was milled through a 200-mesh screen and dried in an oven at 105 °C for 2 h prior to its use in the experiments.

2.2. Preparation of organo-attapulgites

The natural attapulgite was treated with 1.0 mol L⁻¹ HCl for 12 h to prepare acid-activated attapulgite. Then the resulting acid-activated attapulgite was washed by deionized water to neutral pH. The Na-APT was prepared by stirring acid-activated attapulgite for 24 h with a 1.0 mol L⁻¹ aqueous solution of NaCl. Excess NaCl and other exchangeable cations were removed from the exchanged attapulgite by filtering, and it was washed with deionized water until chloride could not be detected using 0.1 mol L⁻¹ AgNO₃. Then Na-APT was dried at 105 °C for 2 h to eliminate the free water and used to prepare organo-attapulgites. Na-APT was characterized with respect to its CEC using an ethylenediamine complex of Cu [30], and the CEC of Na-APT was found as 0.385 mmol g⁻¹, higher than that of natural APT (0.278 mmol g⁻¹).

OTMAC-attapulgite (OTMAC-APT): 2% Na-APT suspension was pretreated by ultrasonic wave to improve the dispersion of Na-APT. The OTMAC was added into the suspension until the ratio of OTMAC/Na-APT was 0.77 mmol g⁻¹. The mixture was

transferred to a microwave reactor, which was equipped with the magnetic stirring system. Then the mixture was stirred and irradiated by microwave at 800 W for 5 min. The final attapulgite was separated from water by vacuum filtration and washed with deionized water for several times until chloride could not be detected using 0.1 mol L⁻¹ AgNO₃. The sample was dried at 80 °C for 4 h and sieved through a 200-mesh screen.

SDS-attapulgite (SDS-APT): SDS was added into 2% Na-APT suspension until the ratio of SDS/Na-APT was 0.77 mmol g⁻¹. The solution pH was adjusted to 1.0 with 0.1 mol L⁻¹ HCl. The reason why the solution pH was adjusted to pH ~1.0 for SDS-APT is to keep the grafted SDS on the surface of attapulgite more stable. Similar method could be seen in the preparation of SDS-montmorillonites [31]. Then the mixture was placed into a microwave reactor. The mixture was stirred and irradiated by microwave at 800 W for 5 min. The final attapulgite was separated from water by vacuum filtration and washed with deionized water for several times. The sample was dried at 80 °C for 4 h and milled through a 200-mesh screen.

OTMAC/SDS-APT: OTMAC and SDS were added into 2% Na-APT suspension simultaneously. The ratios of OTMAC/Na-APT and SDS/Na-APT were 0.77 and 0.385 mmol g⁻¹, respectively. The mixture was put into a microwave reactor and irradiated at 800 W for 5 min. Then the mixture was separated from water by vacuum filtration and washed with deionized water for several times. The sample was dried at 80 °C for 4 h and milled through a 200-mesh screen.

Table 2
Chemical composition of natural attapulgite

Component	MgO	Al ₂ O ₃	SiO ₂	Fe ₂ O ₃	K ₂ O	CaO	Na ₂ O	TiO ₂	MnO
Content (%)	8.66	16.98	62.55	5.83	1.64	1.52	0.35	0.64	0.40

2.3. Material characterization

The elemental analysis (Vario EL III Elemental Analyzer, Germany) was performed to determine the contents of C, N, and S in organo-attapulgites. XRD was performed on a Rigaku D/Max diffractometer with Cu K α radiation ($\lambda = 0.15418$ nm). The diffracted intensities were recorded from 3 to 70 2θ -angles and the XRD device was operated at 40 kV and 100 mA. FT-IR was carried out on FT-IR spectrophotometer (Nicolet 67), using the KBr disk method. The morphology and size of the samples were studied with a field emission scanner (FE-SEM, JEOL JSM-6700F). N₂ adsorption–desorption isotherms (at 77.3 K) were obtained using a Tristar II 3020 automatic surface area and pore analyzer. The adsorption data were then employed to determine surface area using the Brunauer, Emmett, and Teller (BET). Zeta potentials of organo-attapulgites in solid/water suspensions were measured using a Zeta potential analyzer (Zetasizer Nano ZS90, Malvern Co., UK).

2.4. Removal of 1-naphthol by adsorption

The adsorption experiments were carried out under ambient conditions using batch technique in 10 mL glass centrifuge tubes and conducted with aluminum foil-lined Teflon screw caps to prevent degradation of 1-naphthol during adsorption experiments. The stock suspensions of 1-naphthol solution, NaCl solution, and adsorbents were added into the glass centrifuge tubes to achieve the desired concentrations of different components. The pH of the mixed suspensions were adjusted to achieve the desired values by adding negligible volumes of 0.01 or 0.1 mol L⁻¹ HCl or NaOH. The concentration of background electrolyte (NaCl) in each glass centrifuge tube was 0.01 mol L⁻¹. For adsorption kinetic study experiments, the contact time was in the range of 1–120 min and the pH was chose to 6.5 \pm 0.1. For the pH effect experiments, the initial concentration of 1-naphthol was 50 mg L⁻¹ and the initial pH were set over a range of 2–11. For adsorption isotherm experiments, the range of 1-naphthol concentration was 10–150 mg L⁻¹ and the initial pH of the suspensions were adjusted to 6.5 \pm 0.1. Prior to initialing an adsorption experiment, a certain amount of adsorbents was transferred to a glass centrifuge tube to obtain a solid content of 2.0 g L⁻¹. The centrifuge tubes were equilibrated for 120 min in a reciprocating shaker at 150 rpm. After reaching adsorption equilibrium, the glass centrifuge tubes were centrifuged at 9,000 rpm for 30 min to separate the solid from the liquid phases. The supernatant was filtered through 0.45 μ m

cellulose acetate membrane filter and analyzed to determine the concentration of 1-naphthol by UV–vis spectrophotometer, which was operated at the wavelength of 290 nm. The detection limit using this protocol was approximately 0.05 mg L⁻¹.

The amounts of 1-naphthol adsorbed by Na-APT and organo-attapulgites were calculated from the difference between the initial and equilibrium solution concentrations; solid-phase loading of 1-naphthol, q_e (mg g⁻¹) was calculated from the mass balance: $q_e = V(C_0 - C_e)/m$, where C_0 and C_e are the initial concentration and equilibrium concentration (mg L⁻¹), respectively, and m is the added dose of adsorbent (mg), V is the volume of the suspension (mL). The distribution coefficient (K_d (mL g⁻¹) = $(C_0 - C_e) \times V / (C_e \times m)$) were also calculated from the difference between C_e and C_0 . All experimental data were the averages of duplicate or triplicate experiments. The relative errors of the data were about 5%.

2.5. Data analysis

2.5.1. Kinetic study

For kinetic study, three common kinetic models including (1) intraparticle diffusion model, (2) pseudo-first-order model, and (3) pseudo-second-order model have been tested for goodness of fit for the experimental data using the correlation coefficient (R^2) as a measure of the agreement between the experimental data and the three proposed models. Each of the models is briefly discussed below.

The intraparticle diffusion model was used to study the rate of adsorbate adsorption onto adsorbents, and it could be expressed as Eq. (1) [32]:

$$q_t = k_i t^{0.5} + C \quad (1)$$

where t (min) is the contact time, q_t (mg g⁻¹) is the amount of adsorbate adsorbed on adsorbents at time t , C (mg g⁻¹) is a constant, and k_i (mg g⁻¹ min^{-0.5}) is the diffusion rate constant which is obtained from the slope of plot of q_t versus $t^{0.5}$.

The pseudo-first-order model can be written as Eq. (2) [33]:

$$\frac{dq_t}{dt} = k(q_e - q_t) \quad (2)$$

After integration, the linear form of Eq. (2) becomes:

$$\ln(q_e - q_t) = \ln q_e - kt \quad (3)$$

where q_e (mg g^{-1}) is the amount of adsorbate adsorbed on adsorbents at the equilibrium time, k (min^{-1}) is the rate constant of the pseudo-first-order adsorption.

The pseudo-second-order model consists of all the steps of adsorption including external film diffusion, adsorption, and internal particle diffusion, which can be written as Eq. (4) [34]:

$$\frac{t}{q_t} = \frac{1}{Kq_e^2} + \frac{1}{q_e}t \quad (4)$$

where K ($\text{g mg}^{-1} \text{min}^{-1}$) is the pseudo-second-order rate constant. The values of K and q_e can be calculated by plotting t/q_t versus t and extracting information from the least-squares analysis of slope and intercept and substituting into Eq. (4).

2.5.2. Isotherm modeling

Three well-known adsorption models, Langmuir, Freundlich, and linear models were employed to simulate the adsorption isotherms.

The Langmuir isotherm model is commonly used to describe the monolayer adsorption process onto surfaces. Its form can be expressed by the following equation (Eq. (5)) [35]:

$$q_e = \frac{K_L q_m C_e}{1 + K_L C_e} \quad (5)$$

Eq. (5) can be expressed in linear form:

$$C_e/q_e = 1/K_L q_m + C_e/q_m \quad (6)$$

where q_m (mg g^{-1}), the maximum adsorption capacity, is the amount of adsorbate at complete monolayer coverage, q_e (mg g^{-1}) is the equilibrium adsorption capacity, and K_L (L mg^{-1}) is the Langmuir constant that relates to the heat of adsorption process.

The Freundlich isotherm model allows for several kinds of adsorption sites on the solid and represents properly the adsorption data at low and intermediate concentrations on heterogeneous surfaces. The model can be represented by the following equation (Eq. (7)) [36]:

$$q_e = k_F C_e^n \quad (7)$$

Eq. (7) can be expressed in linear form:

$$\log q_e = \log k_F + n \log C_e \quad (8)$$

where k_F ($\text{mg}^{1-n} \text{L}^n \text{g}^{-1}$) represents the adsorption capacity when the equilibrium concentration of adsorbate is equal to 1, and n represents the degree of dependence of adsorption with equilibrium concentration.

The linear form of the linear isotherm model can be presented as Eq. (9):

$$q_e = K_P C_e + b \quad (9)$$

where q_e (mg g^{-1}) is the mass of solute adsorbed per unit mass of adsorbent, C_e (mg L^{-1}) is the equilibrium aqueous-phase solute concentration, K_P (L g^{-1}) is the partition coefficient, and b is a constant.

2.5.3. Thermodynamic study

The thermodynamic parameters (ΔH° , ΔS° , and ΔG°) for adsorbate adsorption on adsorbents can be obtained from the temperature-dependent data. The free energy change (ΔG°) is calculated by Eq. (10):

$$\Delta G^\circ = -RT \ln K_0 \quad (10)$$

where K_0 is the sorption equilibrium constant. Values of $\ln K_0$ are obtained by plotting $\ln K_d$ versus C_e and extrapolating C_e to 0 (K_d is the distribution coefficient) [37]. Its intercept with vertical axis gives the value of $\ln K_0$. Standard entropy change (ΔS°) and average standard enthalpy change (ΔH°) can be calculated from the slope and intercept of the plot of $\ln K_0$ versus $1/T$ using the following equation (Eq. (11)):

$$\ln K_0 = \frac{\Delta S^\circ}{R} - \frac{\Delta H^\circ}{RT} \quad (11)$$

where R ($8.314 \text{ J mol}^{-1} \text{K}^{-1}$) is the ideal gas constant and T (K) is the temperature in Kelvin.

3. Results and discussion

3.1. Characterization of organo-attapulgites

The elemental analysis results of C, N, and S contents for Na-APT, SDS-APT, OTMAC-APT, and OTMAC/SDS-APT are presented in Table 3. It can be found that the C content of Na-APT is 0.25%, which is close to zero, suggesting that the organic carbon is virtually nonexistent. The C contents of the four studied samples increase obviously after modification with OTMAC, SDS, and the mixture of OTMAC and SDS. The C content of SDS-APT (4.24%) is much lower than

Table 3
C, N, and S contents of the organo-attapulgites

Sample	C (%)	N (%)	S (%)	C/N(S)	C/N(S) _{the}
Na-APT	0.25	–	–	–	–
SDS-APT	4.24	–	0.89	4.76	4.49
OTMAC-APT	13.88	0.79	–	17.57	17.99
OTMAC/SDS-APT	14.56	0.67	0.55	21.73 (26.47)	–

Note: C/N(S)_{the}: theoretical value of C/N or C/S.

that of OTMAC-APT (13.88%), suggesting that the SDS molecules are more difficult to be adsorbed on the surface of attapulgite, compared to OTMAC molecules, as the negatively charged SDS has an electrostatic repulsion effect to the negatively charged surface of attapulgite. It is of interest to note that the C content of OTMAC/SDS-APT (14.56%) is higher than that of OTMAC-APT (13.88%). The result suggests that the loading of SDS and synergistic effect between anionic and cationic surfactants make a contribution on the increase in C content of OTMAC/SDS-APT [38]. Moreover, the ratios of C/N for OTMAC-APT and C/S for SDS-APT from elemental analysis results are 17.57 and 4.76, respectively, which are very close to the theoretical values of C/N and C/S. From the N and S contents for SDS-APT, OTMAC-APT, and OTMAC/SDS-APT in Table 2, one can figure out the grafting efficiencies of OTMAC/SDS on the three different samples. Compared with the added surfactants, the grafting efficiencies of OTMAC/SDS on SDS-APT, OTMAC-APT, and OTMAC/SDS-APT are 39.2, 86.3, and 71.8%/51.6%, respectively. From the results, it can be found that the grafting efficiency of SDS on SDS-APT is obviously lower than that of OTMAC on OTMAC-APT. The reason is that the grafted SDS in SDS-APT is less stable than OTMAC in OTMAC-APT at neutral pH [31]. These results confirm that the modification of attapulgite with OTMAC and SDS are accomplished.

The XRD patterns of Na-APT, SDS-APT, OTMAC-APT, and OTMAC/SDS-APT are presented in Fig. 1. It can be observed that attapulgite is the main component phase in the clay used in this study, with appreciable amounts of montmorillonite and quartz. The characteristic *d*-spacing corresponding to (1 1 0), (0 4 0), and (1 6 1) reflections of Na-APT are about 10.5, 4.5, and 2.5 Å, respectively. After organic modification with OTMAC, SDS, and the mixture of OTMAC and SDS, all of the above *d*-spacing values for the attapulgite almost have no change, indicating that the surfactant molecules are only adsorbed on the surface of attapulgite fibers [39,40].

The FT-IR spectra of Na-APT, SDS-APT, OTMAC-APT, and OTMAC/SDS-APT are shown in Fig. 2. In

the FT-IR spectrum of Na-APT, the peaks at 3,620, 3,560, and 3,425 cm⁻¹ correspond to the stretching vibrations of hydroxyl groups in Al–OH, Fe–OH, and zeolitic water, respectively. The peak at 1,655 cm⁻¹ is associated with –OH bending vibration of zeolitic water. The peaks at 1,018 and 475 cm⁻¹ are attributed to Si–O–Si bonds, the peak at 800 cm⁻¹ may be corresponding to the stretching vibration of Al–O–Si [41]. The characteristic peaks appearing around 3,000–2,800 cm⁻¹, due to symmetric and asymmetric stretching of –CH₂ group of organic molecules [42], are observed in the FT-IR spectra of three organo-attapulgites. However, they cannot be found in the spectrum of Na-APT. The results indicate that Na-APT has been modified by surfactants and the surface properties of Na-APT have been changed evidently.

The SEM images of Na-APT, SDS-APT, OTMAC-APT, and OTMAC/SDS-APT are shown in Fig. 3. It can be observed that Na-APT (Fig. 3(A)) presents in the form of dispersive fibers with a high length-diameter ratio. But for the three organo-attapulgites, they present in the form of fiber aggregates and the surfaces of them become rough which are due to the fibers that are bound together by surfactant molecules.

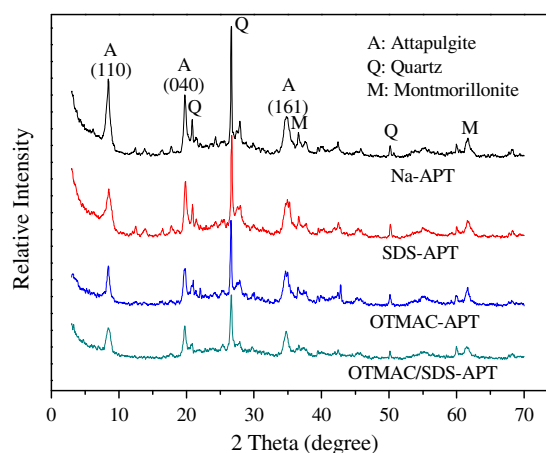


Fig. 1. X-ray patterns of Na-APT, SDS-APT, OTMAC-APT, and OTMAC/SDS-APT.

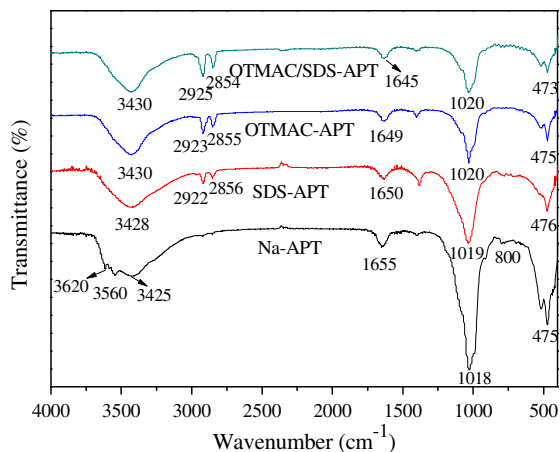


Fig. 2. FT-IR spectra of Na-APT, SDS-APT, OTMAC-APT, and OTMAC/SDS-APT.

The surfactant molecules coating on the surfaces of organo-attapulgites can provide hydrophobic surfaces, which can improve the affinity for hydrophobic organic pollutants.

Fig. 4 shows the N_2 adsorption–desorption isotherms of Na-APT, SDS-APT, OTMAC-APT, and OTMAC/SDS-APT. As can be seen, the isotherms of the four samples are similar and belong to typical type

II in the IUPAC classification [43]. Results for the textural properties are given in Table 4. Compared with Na-APT, the BET surface areas of three organo-attapulgites decrease to different extent. This is attributed to the formation of packed aggregates, which caused by interparticle hydrophobic interactions, and the aggregated structure can be observed by SEM (see Fig. 3). The total pore volumes of the three organo-attapulgites increase due to the formation of a new void in the aggregates. In addition, the pore volumes do not increase proportionally with surface areas which might result in the increase in average pore diameters [28].

The zeta potential can reflect the surface charge properties and electrokinetic properties of solid fine particles in an aqueous solution. As depicted in Fig. 5, the zeta potentials of Na-APT, SDS-APT, OTMAC-APT, and OTMAC/SDS-APT were observed over the pH range of 1.0–11.0, and the pH_{pzc} (point of zero charge) of the four samples were determined by plotting zeta potential values of particulate suspension (2.0 g L^{-1}) versus pH. The zeta potential values of OTMAC-APT at the whole pH range are positive, indicating that there are amounts of positively charged cations coating on the surface of Na-APT. The constantly negative charged value of SDS-APT can be explained by surface modification of SDS as an anionic

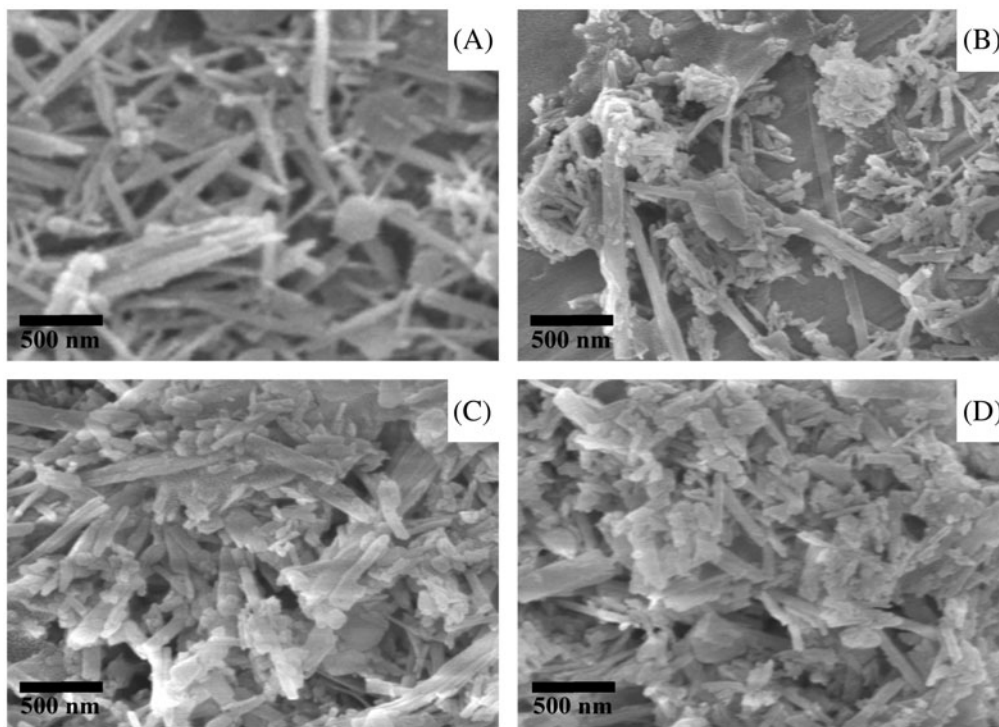


Fig. 3. SEM images of Na-APT (A), SDS-APT (B), OTMAC-APT (C), and OTMAC/SDS-APT (D).

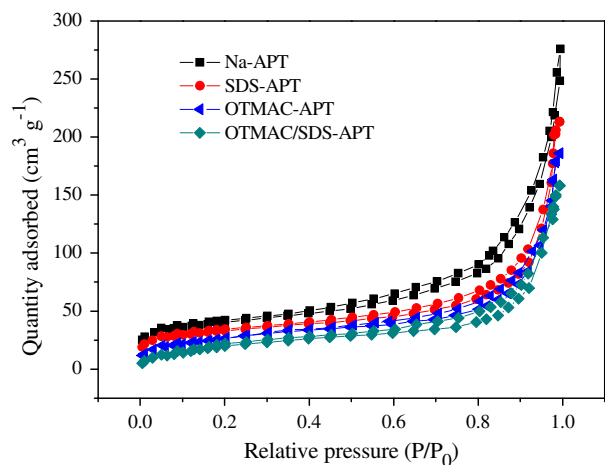


Fig. 4. N_2 adsorption–desorption isothermal curves of Na-APT, SDS-APT, OTMAC-APT, and OTMAC/SDS-APT.

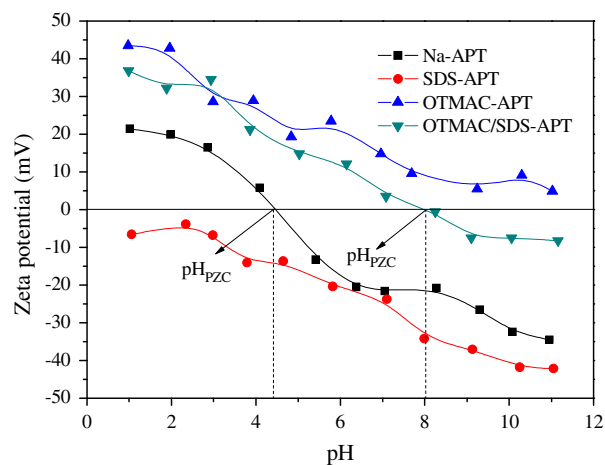


Fig. 5. Zeta potential value as a function of pH for Na-APT, SDS-APT, OTMAC-APT, and OTMAC/SDS-APT (2.0 g L^{-1} suspension).

surfactant, which supplies sulfo group. In the pH range of 1.0–11.0, it can be found that only the pH_{pzc} of Na-APT and OTMAC/SDS-APT can be determined, and the pH_{pzc} of Na-APT and OTMAC/SDS-APT are about 4.5 and 8.0, respectively. The zeta potential values of OTMAC/SDS-APT are always lower than that of OTMAC-APT at the whole pH range. This could be related to the neutralization of SDS, which is negatively charged.

3.2. Effect of initial pH

Solution pH is an important parameter in controlling adsorption process. Fig. 6 shows the effect of initial pH on the adsorption of 1-naphthol on Na-APT, SDS-APT, OTMAC-APT, and OTMAC/SDS-APT. From Fig. 6, it can be observed that the adsorptions of 1-naphthol on the four adsorbents have no significant variations and maintain a high level at the pH range of 2–8 and decrease gradually at $\text{pH} > 8$. This decrement in adsorption due to changes of initial pH, which can be attributed to both the surface charge

behavior of adsorbents and the dissociation chemistry of 1-naphthol changed with initial pH [42].

For attapulgite, the Si–OH and Al–OH groups existing on its external surface are subjected to protonation or deprotonation depending on pH values. In the pH range of 2–11, the Si–OH and Al–OH groups should have a protonation–deprotonation transition, and it appears that such a transition has a significant effect on the adsorptive affinity of attapulgite toward 1-naphthol. At low pH value, the main species of 1-naphthol is neutral nondissociated molecule, while dissociated anion is the main existing species of 1-naphthol at high pH. At high pH, the surfaces of adsorbents can be negatively charged or less positively charged, which can be demonstrated from the zeta potentials of four samples (see Fig. 5). Meanwhile, 1-naphthol can be dissociated to anions when $\text{pH} > \text{pK}_a$ (9.34) [13]. In this way, the electronic repulsion force between the dissociated species of adsorbate and negatively charged adsorbents will result in an adsorption decrease [44]. Sarkar et al. [42] have investigated the effect of pH on adsorption of

Table 4
Textural characteristics of Na-APT, SDS-APT, OTMAC-APT, and OTMAC/SDS-APT

Sample	BET surface area ($\text{m}^2 \text{ g}^{-1}$)	Pore volume ($\text{cm}^3 \text{ g}^{-1}$)	Average pore diameter (nm) ^a
Na-APT	185.86	0.32	6.89
SDS-APT	125.25	0.33	10.54
OTMAC-APT	99.62	0.42	16.86
OTMAC/SDS-APT	78.39	0.39	19.90

^aAverage pore diameter calculated using the relationship $4 \times \text{pore volume}/\text{BET surface area}$.

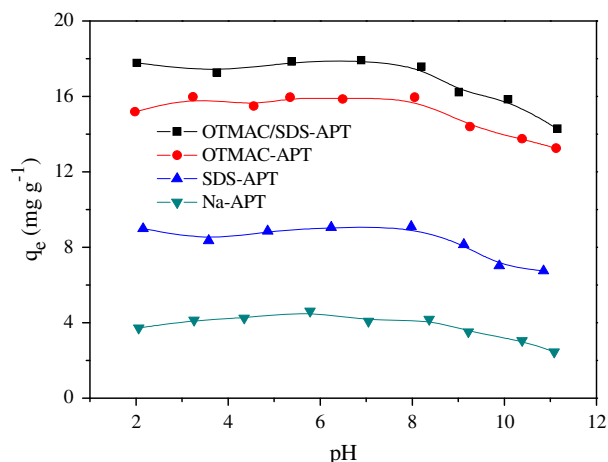


Fig. 6. Adsorption of 1-naphthol on four different adsorbents as a function of initial pH.

organopalygorskites for p-nitrophenol and similar observation was also found.

3.3. Adsorption kinetics

Fig. 7 demonstrates the adsorption kinetics of 1-naphthol on Na-APT, SDS-APT, OTMAC-APT, and OTMAC/SDS-APT. The plots represent the adsorbed 1-naphthol on the four adsorbents versus time at an initial concentration of 50 mg L^{-1} . It can be seen that the adsorption of 1-naphthol on the four adsorbents increase rapidly at the first 10 min of contact time, and then slow down gradually, reach equilibrium at around 60 min, beyond which no significant increase in adsorption can be found.

Three kinetic models, pseudo-first-order model, pseudo-second-order model, and intraparticle diffusion model were applied to simulate the experimental data. According to Eqs. (1), (3), and (4), the linear forms of three kinetic models are shown in Fig. 8 and the corresponding parameters of each kinetic model are presented in Table 5. Based on Fig. 8(A) and Table 5, it can be concluded that the correlation coefficients of the pseudo-second-order equation for 1-naphthol are very close to 1 (>0.995) and greater than that of other two kinetic models, which indicates that the kinetic adsorption of 1-naphthol on the four adsorbents can be well described by the pseudo-second-order model.

For intraparticle diffusion model, the values of k_i and C can be calculated from the slope of the plots of q_t versus $t^{0.5}$ (Eq. (1)). Fig. 8(B) shows that plots of q_t against $t^{0.5}$ consist of two separate linear regions. It can be seen that the correlation coefficients for intraparticle diffusion model are all above 0.94, indicating

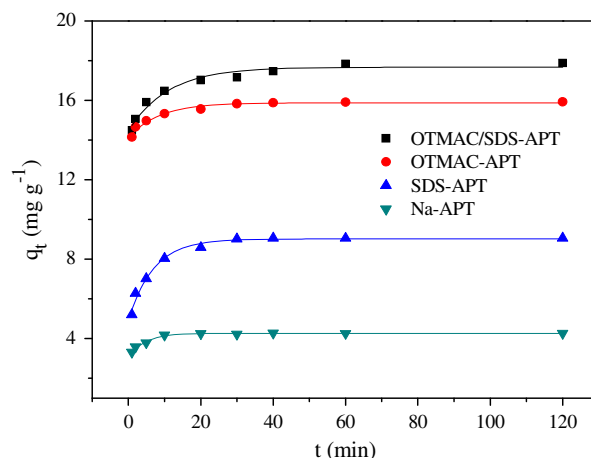


Fig. 7. Adsorption of 1-naphthol on Na-APT, SDS-APT, OTMAC-APT, and OTMAC/SDS-APT as a function of contact time. pH 6.5 ± 0.1 , $C_0 = 50 \text{ mg L}^{-1}$, $m/V = 2.0 \text{ g L}^{-1}$, $T = 298 \text{ K}$, $I = 0.01 \text{ mol L}^{-1}$ NaCl.

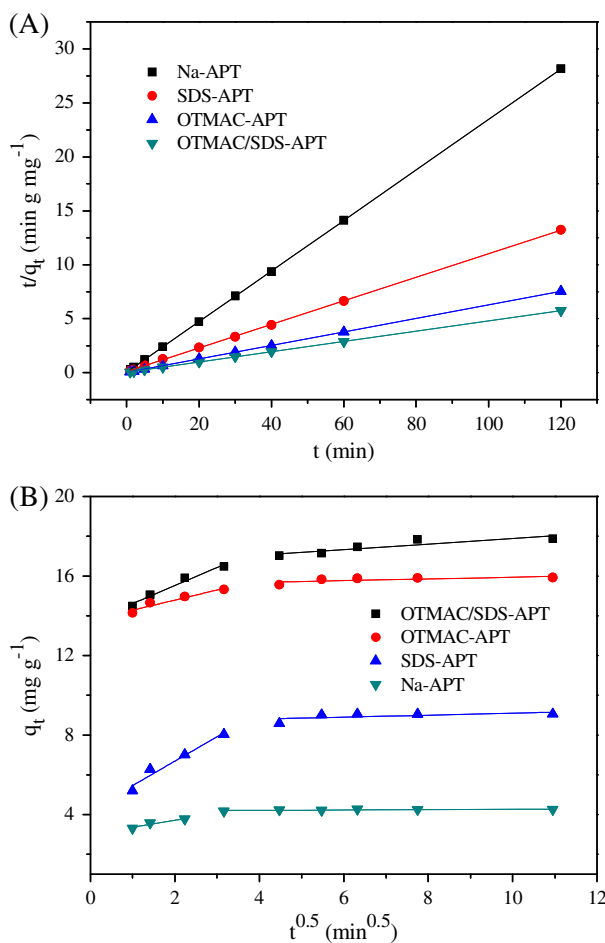


Fig. 8. Pseudo-second-order (A) and intraparticle diffusion (B) plots for the adsorption of 1-naphthol onto Na-APT, SDS-APT, OTMAC-APT, and OTMAC/SDS-APT at 298 K.

Table 5

Kinetic parameters for the adsorption of 1-naphthol on Na-APT, SDS-APT, OTMAC-APT, and OTMAC/SDS-APT

Adsorbents	$q_{e,exp}$	Pseudo-first-order model			Pseudo-second-order model			Intraparticle diffusion model		
		k	$q_{e,cal}$	R^2	K	$q_{e,cal}$	R^2	k_i	C	R^2
Na-APT	4.25	0.09	1.75	0.891	1.15	4.27	0.999	0.605	2.82	0.951
SDS-APT	9.06	0.13	4.23	0.878	0.11	9.16	0.998	0.986	6.05	0.940
OTMAC-APT	15.90	0.11	7.98	0.895	0.23	15.96	0.999	0.852	14.14	0.963
OTMAC/SDS-APT	17.88	0.04	8.56	0.916	0.07	17.98	0.997	0.905	15.08	0.945

that intraparticle diffusion model can also simulate the adsorption of 1-naphthol on the four adsorbents well. The values of intercept show some information about the boundary layer thickness, i.e. the larger the intercept, the greater the boundary layer effect [45]. From Table 5, it can be seen that the values of C are not zero but large values, and the value of C decreases in the order of OTMAC/SDS-APT > OTMAC-APT > SDS-APT > Na-APT. The two separate linear fitting of intraparticle diffusion model also indicates that the kinetics are of typical characteristics of two-step rate control, i.e. at the first stage, the external surface adsorption sites of adsorbents are occupied quickly by 1-naphthol owing to hydrophobic interaction; when the adsorption sites of adsorbents are wholly occupied, the boundary layer diffusion may be the rate-limiting step in the adsorption process for the four adsorbents [46].

Compared with intraparticle diffusion model, pseudo-second-order model, pseudo-first-order model seems to be the worst fitting result from the correlation coefficients listed in Table 5. The rate constant (k_i) and equilibrium adsorption capacity (q_e) of 1-naphthol adsorption by different adsorbents are calculated from the linear plots of $\ln(q_e - q_t)$ versus t (figure not shown) and also listed in Table 5. An obvious difference of equilibrium adsorption capacity (q_e) between the experiment and calculation can be found, which suggests a poor pseudo-first-order fit to the experimental data.

3.4. Equilibrium isotherms

The equilibrium isotherm of adsorption is the most important information, which describes how adsorbate molecules are distributed between the liquid phase and solid phase when the adsorption process reaches equilibrium. Fig. 9 shows the adsorption isotherms of 1-naphthol on Na-APT, SDS-APT, OTMAC-APT, and OTMAC/SDS-APT at three different temperatures, respectively. It can be found that the values of q_e are the lowest at $T = 338$ K and the highest at $T = 298$ K

for four adsorbents, which indicates that the adsorption of 1-naphthol on four adsorbents are enhanced with decreasing temperature.

Langmuir, Freundlich, and linear models were employed to simulate the adsorption isotherms, and the fitting curves are also shown in Fig. 9. According to Eqs. (6), (8), and (9), the fitting parameters derived from the Langmuir, Freundlich, and linear isotherm models are listed in Tables 6–8. From the fitting curves shown in Fig. 9 and the correlation coefficients listed in Tables 6–8, it can be seen that linear model can simulate the experimental data of 1-naphthol adsorption on SDS-APT at three different temperatures best among the three models, while the Langmuir and Freundlich models can simulate the experimental data of 1-naphthol adsorption on Na-APT, OTMAC-APT, and OTMAC/SDS-APT better than linear model. The difference of fitting results among four different adsorbents reveals the different adsorption mechanisms. To the best of our knowledge, there are two adsorption mechanisms, i.e. adsorption and partition, associated with the interfacial behavior of organic compounds in the system of organo-attapulgite/water [26]. The linear and Langmuir type of isotherms are assigned to describe the contribution by partition and adsorption, respectively. The linear model simulates the experimental data of 1-naphthol adsorption on SDS-APT well, suggesting that the adsorption of 1-naphthol on SDS-APT is a linear adsorption process, and the contribution of partition is obviously more than that of adsorption. In contrast to SDS-APT, the adsorption of 1-naphthol on Na-APT, OTMAC-APT, and OTMAC/SDS-APT can be simulated well by Langmuir and Freundlich models, indicating that the adsorption is the dominated effect during the process, and all three adsorbents are covered by a monolayer of 1-naphthol molecules and the surfaces of three adsorbents are heterogeneous. It is worth to note that the correlation coefficients of OTMAC/SDS-APT for three models are very close to one another, revealing that the removal of 1-naphthol by OTMAC/SDS-APT from aqueous solutions is the combination of adsorption and

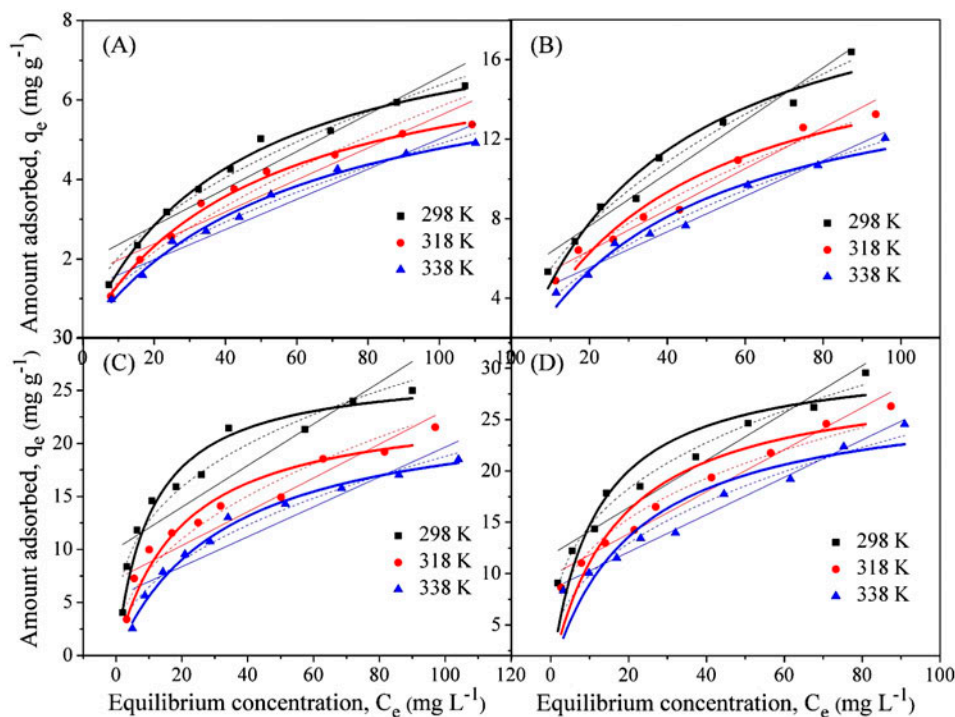


Fig. 9. Adsorption isotherms of 1-naphthol on Na-APT (A), SDS-APT (B), OTMAC-APT (C), and OTMAC/SDS-APT (D) at three different temperatures. Symbols denote experimental data, thick solid lines represent the model fitting of Langmuir equation, dotted lines represent the model fitting of Freundlich equation, and thin solid lines represent the model fitting of linear equation.

partition. From the fitting results of three models, it can be seen that the adsorption of 1-naphthol by organo-attapulgites fits reasonably well to Langmuir, Freundlich, and linear isothermal models, which suggests that the process is controlled by multiple mechanisms.

In addition, from the experimental data shown in Fig. 9 and Langmuir adsorption capacities (q_{\max}) listed in Table 6, the adsorption ability of four adsorbents for 1-naphthol at $T = 298$ K is in the sequence of OTMAC/SDS-APT (31.19 mg g^{-1}) > OTMAC-APT (27.09 mg g^{-1}) > SDS-APT (21.60 mg g^{-1}) > Na-APT (8.70 mg g^{-1}), which is corresponding to the sequence of organic carbon contents of four adsorbents (see Table 3). The results suggest that the organic carbon content has a significant influence on the adsorption ability of four adsorbents toward 1-naphthol. To the best of our knowledge, the surface of attapulgite is hydrophilic, it is natural that attapulgite has little affinity toward hydrophobic 1-naphthol. However, when attapulgite is modified with OTMAC, SDS, and the mixture of OTMAC and SDS, the surface of attapulgite becomes hydrophobic which due to the adsorbed surfactant phases and the hydrophobic interface will have an increasing affinity toward hydropho-

bic organic compounds. Sarkar et al. [42] have studied the adsorption of p-nitrophenol on organopalygorskites, and they found that the adsorption capacities of palygorskites can be greatly improved after modification with dimethyldioctadecylammonium bromide and cetylpyridinium chloride.

In order to verify the feasibility of using OTMAC/SDS-APT as a potential adsorbent for organic wastewater disposal, a comparison of Langmuir adsorption capacity (q_{\max}) of OTMAC/SDS-APT ($q_{\max} = 31.19 \text{ mg g}^{-1}$ for 1-naphthol) studied in this work with that of other common adsorbents such as oxidized MWCNTs ($q_{\max} = 30.58 \text{ mg g}^{-1}$ for 1-naphthol) [13], XC-72 carbon ($q_{\max} = 83.54 \text{ mg g}^{-1}$ for 1-naphthol) [47], and graphene nanosheets ($q_{\max} = 331.59 \text{ mg g}^{-1}$ for 1-naphthol) [14]. Although XC-72 carbon and graphene nanosheets have higher adsorption capacities for 1-naphthol, XC-72 carbon and graphene nanosheets are not able to support wide application because of their high raw material cost or high synthetic cost, as well as its potential ecological toxicity. In contrast, OTMAC/SDS-APT can be easily synthesized by a simple preparation method and has high adsorption capacity for 1-naphthol, no less than oxidized MWCNTs.

Table 6
The parameters for Langmuir isotherms at three different temperatures

Adsorbents	298 K			318 K			338 K		
	q_m	K_L	R^2	q_m	K_L	R^2	q_m	K_L	R^2
Na-APT	8.70	0.024	0.993	7.83	0.021	0.992	7.57	0.017	0.982
SDS-APT	21.60	0.028	0.953	18.19	0.026	0.943	16.41	0.025	0.955
OTMAC-APT	27.09	0.095	0.989	24.02	0.052	0.968	23.90	0.031	0.984
OTMAC/SDS-APT	31.19	0.089	0.971	29.61	0.060	0.959	27.83	0.048	0.961

Table 7
The parameters for Freundlich isotherms at three different temperatures

Adsorbents	298 K			318 K			338 K		
	k_F	n	R^2	k_F	n	R^2	k_F	n	R^2
Na-APT	0.489	0.569	0.972	0.348	0.612	0.960	0.285	0.626	0.979
SDS-APT	1.780	0.490	0.974	1.566	0.471	0.974	1.277	0.488	0.963
OTMAC-APT	4.571	0.406	0.885	2.834	0.453	0.904	1.424	0.582	0.917
OTMAC/SDS-APT	7.323	0.306	0.984	5.713	0.330	0.973	4.937	0.333	0.967

Table 8
The parameters for linear isotherms at three different temperatures

Adsorbents	298 K			318 K			338 K		
	K_P	b	R^2	K_P	b	R^2	K_P	b	R^2
Na-APT	0.047	1.897	0.891	0.040	1.572	0.873	0.038	1.223	0.922
SDS-APT	0.133	4.987	0.989	0.103	4.336	0.986	0.090	3.767	0.972
OTMAC-APT	0.196	10.08	0.760	0.159	7.176	0.870	0.141	5.556	0.856
OTMAC/SDS-APT	0.230	11.82	0.924	0.205	9.774	0.950	0.182	8.454	0.956

3.5. Adsorption thermodynamics

In order to gain insight into the possible mechanisms involved in the removal process, the thermodynamic parameters (ΔH^0 , ΔS^0 , and ΔG^0) were calculated from the adsorption isotherms of 1-naphthol on Na-APT, SDS-APT, OTMAC-APT, and OTMAC/SDS-APT at three different temperatures. The distribution coefficients as a function of solute final concentration at 298, 318, and 338 K are shown in Fig. 10. The values of adsorption equilibrium constant ($\ln K_0$) are obtained by plotting $\ln K_d$ versus C_e and extrapolating C_e to 0, and the intercept is the value of $\ln K_0$ (see Fig. 11). Constants of linear fit of $\ln K_d$ versus C_e for the adsorption of 1-naphthol on Na-APT, SDS-APT, OTMAC-APT, and OTMAC/SDS-APT are listed in Table 9. The slope of Eq. (11) is $\Delta H^0/R$ and the intercept is $\Delta S^0/R$. Thermodynamic parameters calculated from Eqs. (10) to (11) are listed in Table 10.

All the samples present negative standard free energy changes, negative average standard enthalpy changes, and positive standard entropy changes. The negative standard free energy changes indicate that the degree of freedom increases at the solid–liquid interface during the adsorption of 1-naphthol on the four adsorbents. 1-naphthol in solution is surrounded by a tightly bound hydration layer where water molecules are more highly ordered than in the bulk water. When a molecule of 1-naphthol comes into close interaction with the hydration surface of adsorbents, the ordered water molecules in these two hydration layers are compelled and disturbed, thus increasing the entropy of water molecules. Although the adsorption of 1-naphthol molecules on the four adsorbents decreases the degree of freedom of 1-naphthol molecules, it seems likely that positive entropy associated with the adsorption of 1-naphthol on the four

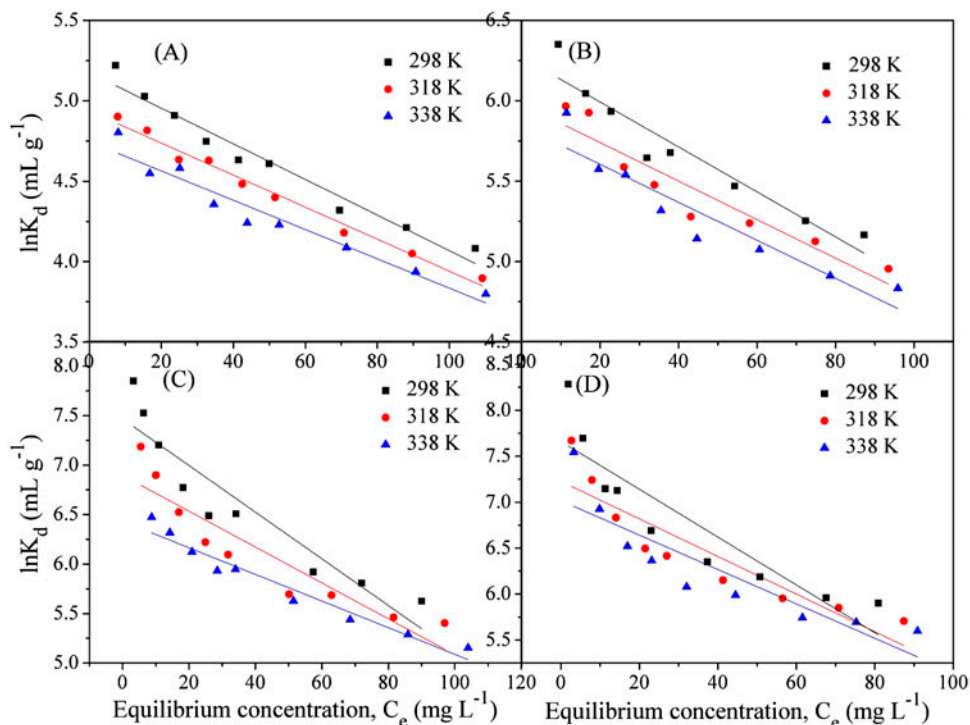


Fig. 10. Linear plots of $\ln K_d$ versus C_e for the adsorption of 1-naphthol on Na-APT (A), SDS-APT (B), OTMAC-APT (C), and OTMAC/SDS-APT (D) at three different temperatures.

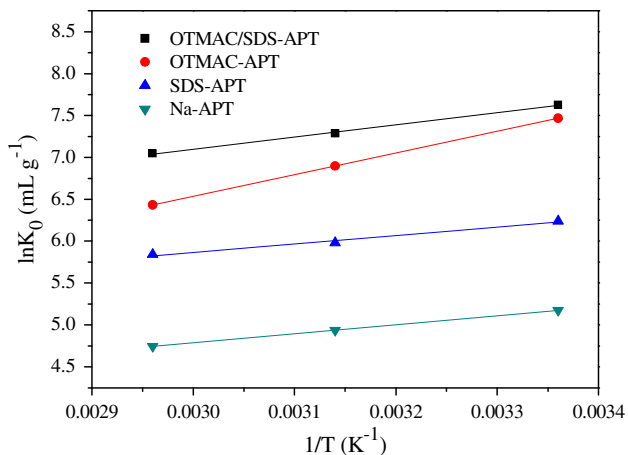


Fig. 11. Linear plots of $\ln K_0$ versus $1/T$ for 1-naphthol adsorption on four adsorbents.

adsorbents is due to the entropy increase in water molecules outweighing the entropy decrease in 1-naphthol molecules [13].

Negative standard free energy changes and negative average standard enthalpy changes indicate that the adsorptions of 1-naphthol on the four adsorbents are general spontaneous and exothermic process. The

absolute values of ΔG° for the four adsorbents at the same temperature are in the sequence of OTMAC/SDS-APT > OTMAC-APT > SDS-APT > Na-APT, indicating that the adsorption process is more favorable when the organic carbon content of the adsorbents is higher. In the adsorption process, the values of binding energy caused by different forces are shown in Table 11 [48]. The negative values of ΔH° (ranging from -15.48 to -8.35 kJ mol^{-1}) also the physical nature of the adsorption process, involving hydrophobic interaction forces, van der Waal's forces, weak forces of electrostatic attraction, dipole bond forces, and hydrogen bond forces [49]. Huang et al. [21] studied the adsorption properties of OTMAC-modified attapulgite for phenol, and similar results were also reported.

3.6. Mechanisms of 1-naphthol removal

By integrating all the above-mentioned analysis together, it can be inferred that the mechanism of 1-naphthol removal is a combination of surface adsorption and partitioning mechanism [26]. But for the four different adsorbents, there are some differences of 1-naphthol adsorption processes according to differences in their active surface properties.

Table 9
 Constants of linear fit of $\ln K_d$ versus C_e ($\ln K_d = B + AC_e$)

Adsorbents	298 K			318 K			338 K		
	A	B	R ²	A	B	R ²	A	B	R ²
Na-APT	-0.011	5.175	0.957	-0.010	4.936	0.984	-0.009	4.746	0.939
SDS-APT	-0.013	6.240	0.905	-0.012	5.980	0.875	-0.012	5.841	0.871
OTMAC-APT	-0.024	7.467	0.858	-0.018	6.897	0.840	-0.013	6.433	0.947
OTMAC/SDS-APT	-0.027	7.720	0.756	-0.021	7.257	0.788	-0.019	7.016	0.761

Table 10
 Thermodynamic parameters of 1-naphthol adsorbed on four adsorbents

Adsorbents	ΔG° (kJ mol ⁻¹)			ΔS° (J mol ⁻¹ K ⁻¹)	ΔH° (kJ mol ⁻¹)
	298 K	318 K	338 K		
Na-APT	-12.82	-13.05	-13.34	13.03	-8.93
SDS-APT	-15.46	-15.81	-16.41	23.74	-8.35
OTMAC-APT	-18.50	-18.23	-18.08	10.09	-15.48
OTMAC/SDS-APT	-18.98	-19.26	-19.80	22.62	-12.13

Table 11
 Values of binding energy caused by different forces

Forces	Hydrophobic interaction forces	van der Waal's forces	Dipole bond forces	Hydrogen bond forces	Chemical adsorption forces
Value of binding energy (kJ mol ⁻¹)	~4	4~10	2~29	2~40	>60

Compared with other three adsorbents, the adsorption of 1-naphthol on OTMAC/SDS-APT is highest. It is known that aluminosilicate minerals modified with cationic surfactants and anionic surfactants such as HDTMA and SDS can substantially enhance the adsorption of ionizable organic solutes from aqueous solutions, because the mixture of anionic and cationic surfactants can form mixed micelles, which can produce synergies solubilization to organic compounds [27]. In this work, one of the interaction mechanisms is described as a hydrophobic partitioning process into the organic solvent-like hydrophobic phase created by the C-18 chain of OTMAC and C-12 chain of SDS. This mechanism is of London-van der Waals type, and is deemed to operate analogously as described by Fig. 12(A). In the case of 1-naphthol removal by OTMAC/SDS-APT, the pH value of the basic solution was 6.5 and the part of 1-naphthol exists as anionic form $C_{10}H_7O^-$. On this basis the ion-dipole interaction between dipole charges of anion $C_{10}H_7O^-$ and nitrogen atoms of head groups of the cationic surfactant (OTMAC) may be considered as a probable

mechanism of 1-naphthol adsorption (see Fig. 12(B)). It is further suggested that, when interacting with each surfactant layer, the hydrophobic benzene ring of 1-naphthol molecules would point to the inside of the hydrophobic phase of OTMAC/SDS, because this orientation allows the hydrophobic interaction between the benzene ring of 1-naphthol and the C-18/C-12 tail of OTMAC/SDS to come about and thus strengthens the retention of 1-naphthol [50]. Moreover, neutral 1-naphthol may also interact with the positively charged head of OTMAC through the oxygen atoms of a phenol compounds capable of donating electrons (Fig. 12(C)), but this coordination interaction would be much weaker than ion-dipole interaction. Another possible interaction mechanism is the hydrogen bonding of 1-naphthol with Si (or Al)-O on attapulgite surfaces (Fig. 12(D)). This interaction mechanism cannot be ignored because Na-APT has the certain adsorption capacity for 1-naphthol from the previous experimental data. The discussions above show four probable interaction models for 1-naphthol removal, where model A represents hydrophobic partitioning

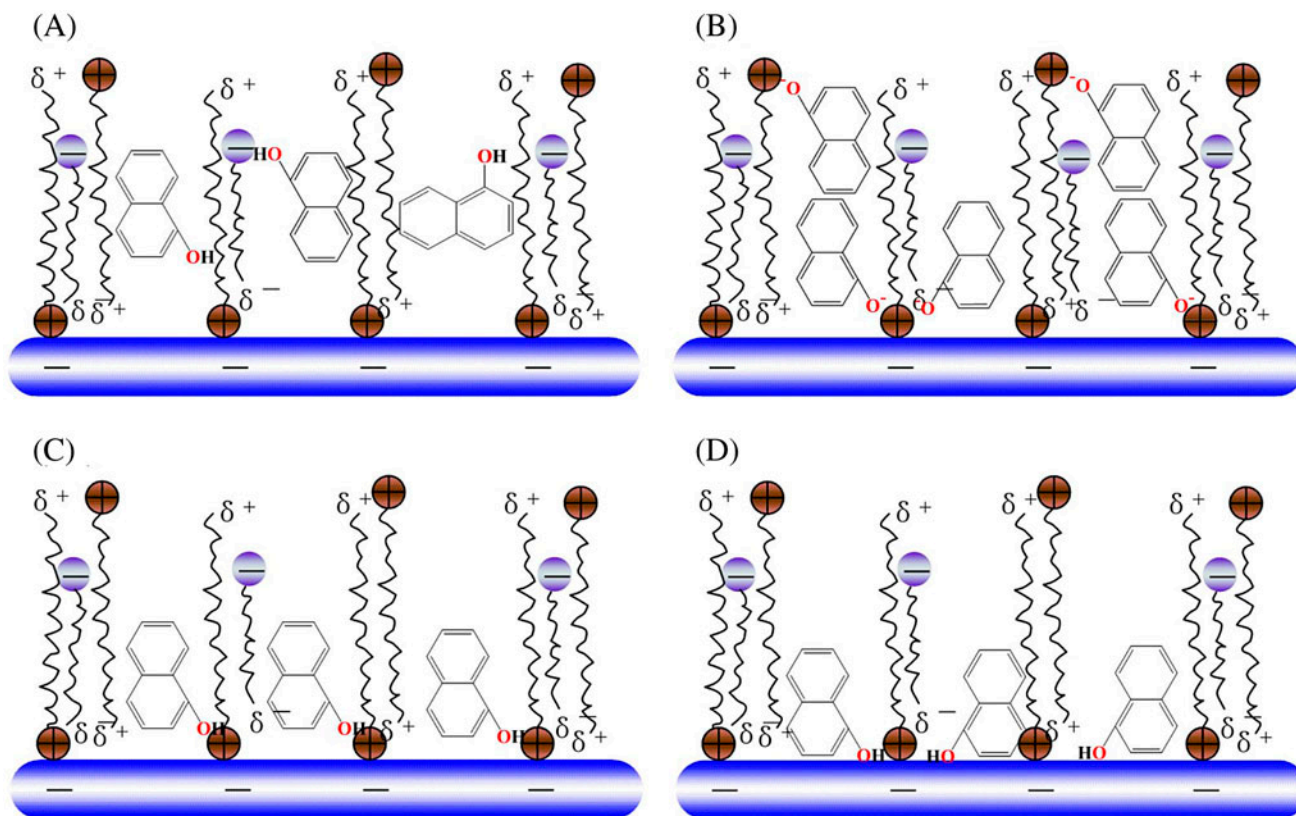


Fig. 12. The probable interaction models of 1-naphthol removal by OTMAC/SDS-APT. (A), (B), (C), and (D) represent four different interaction models.

mechanism, model B represents ion–dipole interaction, model C represents coordination interaction, and model D represents hydrogen bonding interaction.

For OTMAC-APT, the adsorption capacity for 1-naphthol is lower than that of OTMAC/SDS-APT. The difference of adsorption capacity for 1-naphthol may mainly result from partitioning mechanism, i.e. model A in Fig. 12. For SDS-APT, model A and model D may be the possible interaction models for 1-naphthol adsorption because there are no positive nitrogen atoms existing on the surface of SDS-APT. By analyzing and comparing the removal mechanisms for 1-naphthol among the four adsorbents, it can be seen that the organic modification of attapulgite is of significant influence for the removal of 1-naphthol, as an example of ionizable organic pollutants.

4. Conclusions

In summary, the organo-attapulgites were prepared with different surfactants by microwave-assisted technique and characterized by elemental analysis, XRD, FT-IR, SEM, N_2 adsorption–desorption, and zeta

potential technology. The obtained organo-attapulgites were used for the removal of 1-naphthol from aqueous solutions. The experimental results showed that the adsorption of 1-naphthol on the prepared organo-attapulgites were quickly to achieve adsorption equilibrium within 60 min and could be well fitted by pseudo-second-order model and intraparticle diffusion model. The adsorption of 1-naphthol by organo-attapulgites fit reasonably well to Langmuir, Freundlich, and Linear isothermal models, indicating that the process is controlled by multiple mechanisms such as hydrophobic partitioning, ion–dipole interaction, coordination interaction, and hydrogen bonding interaction. Thermodynamic parameters (ΔH° , ΔS° , and ΔG°) calculated from the temperature dependent adsorption isotherms indicated that the adsorption on organo-attapulgites were spontaneous and endothermic processes. By comparing the adsorption capacities for 1-naphthol among different organo-attapulgites, it could be seen that OTMAC/SDS-APT might be a suitable material for the removal of ionizable organic pollutants from aqueous solutions in environmental pollution management.

Acknowledgment

Natural Science Foundation of Anhui Higher Education Institution of China (grant number KJ2012B093) is acknowledged. Suggestions from unknown reviewers to improve the manuscript are also gratefully acknowledged.

References

- [1] W.M. Zhang, C.H. Hong, B.C. Pan, Q.J. Zhang, P.J. Jiang, K. Jia, Sorption enhancement of 1-naphthol onto a hydrophilic hyper-cross-linked polymer resin, *J. Hazard. Mater.* 163 (2009) 53–57.
- [2] H. Ashraf, Q. Husain, Removal of α -naphthol and other phenolic compounds from polluted water by white radish (*Raphanus sativus*) peroxidase in the presence of an additive, polyethylene glycol, *Biotechnol. Bioprocess Eng.* 14 (2009) 536–542.
- [3] F.X. Xu, D.E. Koch, I.C. Kong, R.P. Hunter, A. Bhandari, Peroxidase-mediated oxidative coupling of 1-naphthol: Characterization of polymerization products, *Water Res.* 39 (2005) 2358–2368.
- [4] Z.J. Hu, N.X. Wang, J. Tan, J.Q. Chen, W.Y. Zhong, Kinetic and equilibrium of cefradine adsorption onto peanut husk, *Desalin. Water Treat.* 37 (2012) 160–168.
- [5] S.T. Yang, Z.Q. Guo, G.D. Sheng, X.K. Wang, Investigation of the sequestration mechanisms of Cd(II) and 1-naphthol on discharged multi-walled carbon nanotubes in aqueous environment, *Sci. Total. Environ.* 420 (2012) 214–221.
- [6] J.Q. Chen, Z.J. Hu, R. Ji, Removal of carbofuran from aqueous solution by orange peel, *Desalin. Water Treat.* 49 (2012) 106–114.
- [7] H.Q. Sun, S.Z. Liu, G.L. Zhou, H.M. Ang, M.O. Tadé, S.B. Wang, Reduced graphene oxide for catalytic oxidation of aqueous organic pollutants, *ACS Appl. Mater. Interfaces* 4 (2012) 5466–5471.
- [8] W.C. Peng, S.Z. Liu, H.Q. Sun, Y.J. Yao, L.J. Zhi, S.B. Wang, Synthesis of porous reduced graphene oxide as metal-free carbon for adsorption and catalytic oxidation of organics in water, *J. Mater. Chem. A* 1 (2013) 5854–5859.
- [9] C. Karunakaran, S. Narayanan, P. Gomathisankar, Photocatalytic degradation of 1-naphthol by oxide ceramics with added bacterial disinfection, *J. Hazard. Mater.* 181 (2010) 708–715.
- [10] S.Y. Zang, B. Lian, J. Wang, Y.J. Yang, Biodegradation of 2-naphthol and its metabolites by coupling *Aspergillus niger* with *Bacillus subtilis*, *J. Environ. Sci.* 22 (2010) 669–674.
- [11] J. Su, H.F. Lin, Q.P. Wang, Z.M. Xie, Z.L. Chen, Adsorption of phenol from aqueous solutions by organomontmorillonite, *Desalination* 269 (2011) 163–169.
- [12] M. Anbia, S.E. Moradi, The examination of surface chemistry and porosity of carbon nanostructured adsorbents for 1-naphthol removal from petrochemical wastewater streams, *Korean. J. Chem. Eng.* 29 (2012) 743–749.
- [13] G.D. Sheng, D.D. Shao, X.M. Ren, X.Q. Wang, J.X. Li, Y.X. Chen, X.K. Wang, Kinetics and thermodynamics of adsorption of ionizable aromatic compounds from aqueous solutions by as-prepared and oxidized multi-walled carbon nanotubes, *J. Hazard. Mater.* 178 (2010) 505–516.
- [14] G.X. Zhao, J.X. Li, X.K. Wang, Kinetic and thermodynamic study of 1-naphthol adsorption from aqueous solution to sulfonated graphene nanosheets, *Chem. Eng. J.* 173 (2011) 185–190.
- [15] S.D. Miao, Z.M. Liu, Z.F. Zhang, B.X. Han, Z.J. Miao, K.L. Ding, G.M. An, Ionic liquid-assisted immobilization of Rh on attapulgite and its application in cyclohexene hydrogenation, *J. Phys. Chem. C* 111 (2007) 2185–2190.
- [16] H. Chen, Y.G. Zhao, A.Q. Wang, Removal of Cu(II) from aqueous solution by adsorption onto acid-activated palygorskite, *J. Hazard. Mater.* 149 (2007) 346–354.
- [17] Q.H. Fan, X.L. Tan, J.X. Li, X.K. Wang, W.S. Wu, G. Montavon, Sorption of Eu(III) on attapulgite studied by batch, XPS, and EXAFS techniques, *Environ. Sci. Technol.* 43 (2009) 5776–5782.
- [18] H. Chen, J. Zhao, A.G. Zhong, Y.X. Jin, Removal capacity and adsorption mechanism of heat-treated palygorskite clay for methylene blue, *Chem. Eng. J.* 174 (2011) 143–150.
- [19] X. Wang, J.M. Pan, W. Guan, X.H. Zou, W. Hu, Y.S. Yan, C.X. Li, Adsorptive removal of 2,6-dichlorophenol from aqueous solution by surfactant-modified palygorskite sorbents: Equilibrium, kinetics and thermodynamics, *Adsorpt. Sci. Technol.* 29 (2011) 185–196.
- [20] M.S. Rodríguez-Cruz, M.S. Andrades, M.J. Sánchez-Martín, Significance of the long-chain organic cation structure in the sorption of the penconazole and metaxyl fungicides by organo clays, *J. Hazard. Mater.* 160 (2008) 200–207.
- [21] J.H. Huang, X.G. Wang, Q.Z. Jin, Y.F. Liu, Y. Wang, Removal of phenol from aqueous solution by adsorption onto OTMAC-modified attapulgite, *J. Environ. Manage.* 84 (2007) 229–236.
- [22] S.D. Haigh, A review of the interaction of surfactants with organic contaminants in soil, *Sci. Total Environ.* 185 (1996) 161–170.
- [23] X.L. Tan, M. Fang, C.L. Chen, S.M. Yu, X.K. Wang, Counterion effects of nickel and sodium dodecylbenzene sulfonate adsorption to multiwalled carbon nanotubes in aqueous solution, *Carbon* 46 (2008) 1741–1750.
- [24] J.X. Li, S.Y. Chen, G.D. Sheng, J. Hu, X.L. Tan, X.K. Wang, Effect of surfactants on Pb(II) adsorption from aqueous solutions using oxidized multiwall carbon nanotubes, *Chem. Eng. J.* 166 (2011) 551–558.
- [25] B. Sarkar, M. Megharaj, Y.F. Xi, R. Naidu, Surface charge characteristics of organo-palygorskites and adsorption of p-nitrophenol in flow-through reactor system, *Chem. Eng. J.* 185–186 (2012) 35–43.
- [26] L.Z. Zhu, B.L. Chen, Sorption behavior of p-nitrophenol on the interface between anion-cationic organobentonite and water, *Environ. Sci. Technol.* 34 (2000) 2997–3002.
- [27] Y. Chang, X.Q. Lv, F. Zha, Y.G. Wang, Z.Q. Lei, Sorption of p-nitrophenol by anion-cation modified palygorskite, *J. Hazard. Mater.* 168 (2009) 826–831.
- [28] A.S. Bhatt, P.L. Sakaria, M. Vasudevan, R.R. Pawar, N. Sudheesh, H.C. Bajaj, H.M. Mody, Adsorption of an anionic dye from aqueous medium by organoclays: Equilibrium modeling, kinetic and thermodynamic exploration, *RSC Adv.* 2 (2012) 8663–8671.

- [29] S.M. Li, Y.L. Wang, M.G. Ma, J.F. Zhu, R.C. Sun, F. Xu, Microwave-assisted method for the synthesis of cellulose-based composites and their thermal transformation to Mn_2O_3 , *Ind. Crops. Prod.* 43 (2013) 751–756.
- [30] F. Bergaya, M. Vayer, CEC of clays: Measurement by adsorption of a copper ethylenediamine complex, *Appl. Clay Sci.* 12 (1997) 275–280.
- [31] P.X. Wu, Y.P. Dai, H. Long, N.W. Zhu, P. Li, J.H. Wu, Z. Dang, Characterization of organo-montmorillonites and comparison for Sr(II) removal: Equilibrium and kinetic studies, *Chem. Eng. J.* 191 (2012) 288–296.
- [32] W. Weber, J. Morris, Kinetics of adsorption on carbon from solution, *J. Sanit. Eng. Div. Am. Soc. Civ. Eng.* 89 (1963) 31–60.
- [33] S.Y. Lagergren, Zur theorie der sogenannten adsorption gelöster stoffe (About the theory of so-called adsorption of soluble substances), *Kungliga Svenska Vetenskapsakademiens Handlingar* 24 (1898) 1–39.
- [34] Y.S. Ho, G. McKay, Pseudo-second order model for sorption processes, *Process Biochem.* 34 (1999) 451–465.
- [35] I. Langmuir, The adsorption of gases on plane surfaces of glass, mica and platinum, *J. Am. Chem. Soc.* 40 (1918) 1361–1403.
- [36] H.M.F. Freundlich, Über die adsorption in Lösungen, *Z. Phys. Chem. (Leipzig)* 57 (1906) 385–470.
- [37] S.T. Yang, J.X. Li, Y. Lu, Y.X. Chen, X.K. Wang, Sorption of Ni(II) on GMZ bentonite: Effects of pH, ionic strength, foreign ions, humic acid and temperature, *Appl. Radiat. Isotopes* 67 (2009) 1600–1608.
- [38] D. Chen, J.X. Zhu, P. Yuan, S.J. Yang, T.H. Chen, H.P. He, Preparation and characterization of anion-cation surfactants modified montmorillonite, *J. Therm. Anal. Calorim.* 94 (2008) 841–848.
- [39] H. Chen, J. Zhao, Adsorption study for removal of Congo red anionic dye using organo-attapulgite, *Adsorption* 15 (2009) 381–389.
- [40] J.H. Huang, Y.F. Liu, Q.Z. Jin, X.G. Wang, J. Yang, Adsorption studies of a water soluble dye, Reactive Red MF-3B, using sonication-surfactant-modified attapulgite clay, *J. Hazard. Mater.* 143 (2007) 541–548.
- [41] Q.H. Fan, D.D. Shao, J. Hu, W.S. Wu, X.K. Wang, Comparison of Ni^{2+} sorption to bare and ACT-graft attapulgites: Effect of pH, temperature and foreign ions, *Surf. Sci.* 602 (2008) 778–785.
- [42] B. Sarkar, Y.F. Xi, M. Megharaj, G.S.R. Krishnamurti, R. Naidu, Synthesis and characterisation of novel organopalygorskites for removal of p-nitrophenol from aqueous solution: Isothermal studies, *J. Colloid Interface Sci.* 350 (2010) 295–304.
- [43] B.D. Zdravkov, J.J. Čermák, M. Šefara, J. Janků, Pore classification in the characterization of porous materials: A perspective, *Cent. Eur. J. Chem.* 5 (2007) 385–395.
- [44] X. Yang, J.X. Li, T. Wen, X.M. Ren, Y.S. Huang, X.K. Wang, Adsorption of naphthalene and its derivatives on magnetic graphene composites and the mechanism investigation, *Colloids Surf., A* 422 (2013) 118–125.
- [45] N. Kannan, M.M. Sundaram, Kinetics and mechanism of removal of methylene blue by adsorption on various carbons—A comparative study, *Dyes Pigm.* 51 (1) (2003) 25–40.
- [46] A.S. Özcan, A. Özcan, Adsorption of acid dyes from aqueous solutions onto acid-activated bentonite, *J. Colloid Interface Sci.* 276 (1) (2004) 39–46.
- [47] L.M. Zuo, S.M. Yu, L.L. Cheng, E.L. Du, Adsorption of phenol and 1-naphthol onto XC-72 carbon, *Korean J. Chem. Eng.* 30(3) (2013) 714–723.
- [48] B.V. von Oepen, W. Kördel, W. Klein, Sorption of nonpolar and polar compounds to soils: Processes, measurements and experience with the applicability of the modified OECD-Guideline 106, *Chemosphere* 22 (1991) 285–304.
- [49] P.X. Wu, Z.W. Liao, H.F. Zhang, J.G. Guo, Adsorption of phenol on inorganic-organic pillared montmorillonite in polluted water, *Environ. Int.* 26 (2001) 401–407.
- [50] Y. Dong, D.Y. Wu, X.C. Chen, Y. Lin, Adsorption of bisphenol A from water by surfactant-modified zeolite, *J. Colloid Interface Sci.* 348 (2010) 585–590.